Stem Cell & Translational Investigation 2015; 2: e1017. doi: 10.14800/scti.1017; © 2015 by Stéphanie Lecaudé, *et al*.
http://www.smartscitech.com/index.php/scti

RESEARCH ARTICLE

Bone marrow-derived stem cells differentiate into retinal pigment epithelium-like cells *in vitro* but are not able to repair retinal degeneration *in vivo*

Stéphanie Lecaudé[1,2], Ute E.K. Wolf-Schnurrbusch[1], Hannan Abdillahi[3], Volker Enzmann[1,2]

[1]*Department of Ophthalmology, Inselspital, Bern University Hospital, University of Bern, Bern, Switzerland*
[2]*Department of Clinical Research, University of Bern, Bern, Switzerland*
[3]*Bern Photographic Reading Center, Inselspital, Bern University Hospital, University of Bern, Switzerland*

Correspondence: Volker Enzmann
E-mail: volker.enzmann@insel.ch
Received: September 15, 2015
Published online: October 15, 2015

The bone marrow (BM) is home to different stem/progenitor populations, including tissue-committed stem cells. In this context, we have cocultured BM-derived stem cells (BMSC) in order to investigate their differentiation capacity towards the retinal pigment epithelial (RPE) lineage *in vitro*. Furthermore, pre-differentiated BMSC were transplanted into the pharmacologically damaged subretinal space to determine their rescue ability *in vivo*. BM was harvested from the tibias and femurs of adult GFP$^+$ C57BL/6 mice. Differentiated hematopoietic cells were removed by lineage depletion, and CD45$^-$ BMSCs were separated by magnetic activated cell sorting (MACS). To induce differentiation, the cells were then cocultured with murine RPE for 10 days, and retinal markers were assessed using immunohistochemistry (IHC). To induce retinal degeneration, mice were treated with sodium iodate ($NaIO_3$). Seven days later, approx. 60,000 pre-differentiated GFP$^+$ BMSC, sorted by FACS, were transplanted subretinally. Optical coherence tomography (OCT) was used to follow the transplants and to quantify the retinal thickness over time. Visual acuity was measured concurrently using the optokinetic reflex (OKR). Finally, IHC was performed to investigate the expression of retina-specific markers in the transplants. CD45$^-$ BMSC adopted an RPE-like elongated morphology and showed expression of the RPE markers RPE65 and bestrophin after coculture. After transplantation of CD45$^-$ BMSC, visual acuity increased in individual animals compared to the contralateral control eye, but did not reach baseline levels. Additionally, no significant increase in retinal thickness in the transplanted eye was found. However, the cells were detectable in the subretinal space for up to 28 days and expressed the RPE markers RPE65 and bestrophin. In summary, the BMSC differentiated into RPE-like cells but were not able to restore visual function or rescue retinal morphology after subretinal transplantation.

Keywords: retina; degeneration; sodium iodate; transplantation; differentiation; bone marrow-derived stem cells

To cite this article: Stéphanie Lecaudé, *et al*. Bone marrow-derived stem cells differentiate into retinal pigment epithelium-like cells *in vitro* but are not able to repair retinal degeneration *in vivo*. Stem Cell Transl Investig 2015; 2: e1017. doi: 10.14800/scti.1017.

Introduction

Replacement of the degenerated retinal pigment epithelium (RPE) before irreversible degeneration of the foveal photoreceptors occurs was considered as a potential therapy for age-related macular degeneration (AMD) nearly 20 years ago [1]. However, several experimental and clinical trials since then have shown that allogeneic RPE cells were

not able to attach and fail to fill in the atrophic area under pathological conditions [2, 3]. Autologous RPE cell transplantation did also not show evidence of functional recovery [4, 5]. In order to achieve more effective regeneration of the damaged retinal structures stem cells (SC) have come into the focus.

New findings have recently contradicted the central dogmas of commitment of adult SC, including bone marrow-derived stem cells (BMSCs), by showing their plasticity to differentiate across tissue-lineage boundaries, irrespective of classical germ layer designations [6]. In this context transdifferentiation into non-hematopoietic, including retinal, cell types was documented [7-9]. The bone marrow contains several subsets of SCs including hematopoietic stem cells providing all blood cell types, non-hematopoietic mesenchymal stem cells that differentiate into mesenchymal tissue and a population of tissue-committed SCs. The existence of these already committed SCs has increased research in the differentiation capacity of adult BMSCs for autologous regeneration purposes [10]. Indeed, a subset of Lin^- $Sca\text{-}1^+$ $CD45^-$ BMSCs that express markers of ocular (retina/RPE) progenitors have been identified and isolated [11]. Furthermore, BMSCs can be triggered to commit to and progress along the RPE differentiation pathway in culture [12]. BMSCs also home to the subretinal space if systemically transferred or endogenously mobilized where they express RPE lineage markers [13-15].

Pre-differentiation of SC *in vitro* using extrinsic factors and/or coculturing is thereby a possible way not only to commit the cells towards a distinctive fate but also to enhance their properties and possibly the outcome of regenerative approaches [16, 17]. Therefore, we have investigated the potential of Lin^- $CD45^-$ BMSCs to be pre-committed towards the RPE lineage *in vitro* and to morphologically and functionally regenerate damaged retinal tissue after subretinal transplantation. To quantify potential rescue effects *in vivo*, we have used the sodium iodate ($NaIO_3$) model of retinal degeneration [18]. $NaIO_3$ is specifically toxic for the RPE, triggering damage to photoreceptors and the choriocapillaris in a dose- and time-dependent manner [19, 20]. The deleterious effects of $NaIO_3$ on the different retinal cell types can also be linked to the impairment of functional visual behavior [21].

Herein, we present evidence that $CD45^-$ BMSCs express RPE markers after coculture with adult RPE but cannot restore visual function completely or rebuild retinal structures that were damaged during retinal degeneration. Further investigation into the potential use of BMSCs to replace degenerated cells for the repair of degenerative changes in the retina is therefore necessary.

Materials and methods:

Cell preparation

All animal experiments were conducted according to the ARVO Statement for the Use of Animals in Ophthalmic and Vision Research following governmental approval. BMSCs were obtained from 3–4-week-old GFP^+ mice (C57BL/6-Tg(UBC-GFP)30Scha/J, Stock Number: 4353). Full bone marrow from a minimum of eight animals was harvested from the femurs and tibias, and magnetic activated cell separation (MACS™) was used for separation according to the manufacturer's recommendations. In short, initial lineage depletion (Lineage Cell Depletion Kit, mouse; Miltenyi Biotec, Bergisch Gladbach, Germany) was performed on LS separation columns. This was followed by separation of Lin^- $CD45^+$ cells (CD45 Micro Beads, mouse; Miltenyi Biotec) on MS separation columns. Lineage-negative cells represented 1.52 ± 0.01% of the total bone marrow cell population. Further separation yielded 48.70 ± 0.18% $CD45^-$ BMSCs of the entire lineage-negative fraction.

Murine adult RPE were enzymatically prepared from 10-day-old C57BL/6 mice. Thereby, the eyes were enucleated, washed, and incubated in dispase for 25 min at 37°C. The anterior part of the eye, lens and sensory retina was then discarded and the RPE mechanically harvested. The cells were plated in DMEM + 10% fetal calf serum + 0.1% antibiotic-antimycotic solution (Life Technologies) for long-term cell culture (maximum five passages).

Coculture of BMSC

The isolated GFP^+ $CD45^-$ BMSCs were grown in coculture with RPE in 0.1% gelatin-coated culture vessels at a 1:1 ratio for up to 10 days with 35,000 cells/well in an eight-well chamber slide (Lab-Tek II; Sigma-Aldrich) or 100,000 cells/well in a six-well plate (Greiner Bio-One, Frickenhausen, Germany). To inhibit proliferation, the feeder cells were treated with mitomycin C for 20 min (50 µg/ml; Sigma-Aldrich) before coculture. Every three days, half of the differentiation medium [DMEM + GlutaMAX with 10% fetal calf serum (Life Technologies), 1% cell shield (Minerva Biolabs, Berlin, Germany), and 10 µM Rock inhibitor Y-27632 (Sigma-Aldrich; for the first 3 days only)] was changed. The cocultures were then either characterized by immunohistochemistry (IHC) or separated by FACS for transplantation purposes (see below).

Immunohistochemistry

Table 1. List of primary antibodies used for immunohistochemistry to identify the *in vitro* differentiation and the cell fate after transplantation *in vivo*

Antigen	Product code / Clone	Company	Origin	Dilution
III- tubulin	ab18207 / n.a.	Abcam	rabbit	1:250
MAP-2	ab11267 / HM-2	Abcam	mouse	1:200
GFAP	ab10062 / GF5	Abcam	rabbit	1:200
RPE65	MA1-16578 / 401.8B11.3D9	ThermoFisher	mouse	1:100
Bestrophin	ab14927 / n.a.	Abcam	rabbit	1:100

n.a. not applicable

After 10 days of coculture in eight-well chamber slides, the cells were fixed with 4% paraformaldehyde (PFA) at room temperature (RT) for 15 min. The samples were then blocked by 3% normal goat serum in PBS with 0.1% Tween 20 at RT for 30 min and incubated with primary antibodies against retina-specific markers (Table 1) at 4°C overnight. Afterwards, the samples were incubated at RT with the appropriate secondary antibody [goat anti-mouse/rabbit Alexa594 (Life Technologies) 1:1000] for 1 h. Finally, the slides were mounted with **V**ectashield Mounting Medium containing DAPI (DAPI H-1200; Vector Labs, Burlingame, CA, USA).

IHC was also performed to evaluate BMSC differentiation after transplantation (see below). For this, 5-µm-thick paraffin retina sections were boiled in Tris EDTA pH 9.0 + 0.05% Tween 20 in a pressure cooker for 3 min. Nonspecific binding was blocked with 10% normal goat serum + 1% bovine serum albumin in Tris-buffered saline + 0.025% Triton 100 (Life Technologies) at pH 7.6 in a humidity chamber at RT for 2 h. The sections were then incubated with marker-specific primary antibodies at 4°C overnight (Table 1). After washing, the sections were incubated with secondary antibodies (see above) at RT for 45 min. This was followed by consecutive staining for GFP, beginning with blocking with 3% normal mouse serum at RT for 1 h, and followed by the primary antibody [chicken anti-GFP (Abcam) 1:500] incubation at 4°C overnight. After washing, the sections were incubated with secondary antibodies [goat anti-chicken Alexa488 (Life Technologies) 1:1000] at RT for 45 min and mounted with **V**ectashield (Vector Labs).

FACS sorting

The cells were detached from six-well tissue culture plates using a non-enzymatic dissociation solution (Sigma-Aldrich) at coculture day 10. GFP^+ BMSCs were separated from the feeder cells by fluorescence activated cell sorting (FACS) using a BD FACSAria™ (Becton Dickinson, Mountainview, CA, USA). In order to segregate the different cell populations, the samples were gated according to their side scatter (SSC) and forward scatter (FSC) pattern using cultured RPE and bone marrow cells as controls. Propidium iodide (PI; Sigma-Aldrich) was used to exclude dead cells and the FL1 fluorescence channel to select GFP^+ cells. The sorting strategy has been visualized in supplemental figure S1.

Subretinal transplantation in the $NaIO_3$ model

Six- to eight-week-old male C57BL/6 mice (Charles River WIGA, Sulzfeld, Germany) received a single i.v. injection of sterile 0.5% sodium iodate ($NaIO_3$; Sigma-Aldrich) in saline (final concentration: 15 mg/kg body weight) or 100 µl 0.9% NaCl. In correlation with the kinetics of the $NaIO_3$-induced degeneration, pre-differentiated GFP^+ BMSCs in balanced salt solution (BSS; Alcon; Hünenberg, Switzerland) were transplanted into the subretinal space of the right eyes 7 days after the initiation of retinal degeneration. The left eyes served as controls and received a similar volume of BSS. Before surgery, pupils were dilated by topical instillation of 2.5% phenylephrine + 0.5% tropicamide (MIX eye drops; ISPI, Bern, Switzerland), and the animals were anesthetized with 2% isoflurane (Forene; Abbott, Baar, Switzerland). Oxybuprocaine (Novesin 0.4%; OmniVision, Neuhausen, Switzerland) was used for local anesthesia. The cells were delivered to the subretinal space by a scleral approach using a Hamilton syringe with a 30-gauge RN needle (Hamilton, Bonaduz, Switzerland). The procedure was performed under sterile conditions using a surgical microscope and a coverslip on hydroxypropyl methylcellulose (Methocel 2%, OmniVision) to adjust the refractive power.

Transplant imaging and retinal thickness measurement

To visualize location and fate of the transplants over time, fundus autofluorescence (FAF) and optical coherence tomography (OCT) images were recorded on day 7, 14, 21, and 28 post transplantation (PT). For that, the animals received general anesthesia using subcutaneous injection of 80 mg/kg ketamine (Ketalar 50 mg/ml; Pfizer, Zurich, Switzerland) and 1 mg/kg medetomidine (Domitor 1 mg/ml;

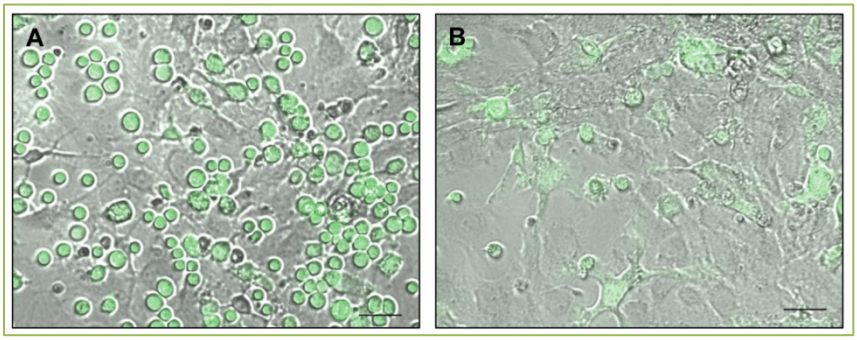

Figure 1. Phenotypical changes in BMSC during coculture with mouse RPE over time. Shown are representative images of GFP^+ BMSCs changing their morphology from a small, round appearance to a more elongated, epithelial-like shape at different time points in coculture. A) culture day 3 and B) culture day 10. Bar represents 50 μm.

Orion Pharma, Espoo, Finland). Pupils were dilated with 2.5% phenylephrine + 0.5% tropicamide (MIX eye drops; ISPI). Methylcellulose (Methocel 2%; OmniVision, Neuhausen, Switzerland) in combination with a contact lens (Quantum I; Bausch + Lomb, Rochester, NY, USA) was used to effectively correct the refractive power of the air–corneal interface and to avoid corneal dehydration. A 78D double-aspheric fundus lens (Volk Optical, Inc., Mentor, OH) was used to adapt the mouse optics to the Spectralis HRA+OCT device (Heidelberg Engineering, Heidelberg, Germany). The anesthesia was revoked by atipamezole (Antisedan 5 mg/ml; Orion Pharma).

The system allows for simultaneous recording of OCT scans with infrared (IR; excitation wavelength: 513 nm) and FAF (excitation wavelength: 488 nm) images. The IR and FAF images were obtained in accordance with a standardized operation protocol, whereas the OCT imaging was performed by manually adjusting the length of the reference pathway using the "OCT debug window" to adjust for the optical length of the scanning pathway. Ring-like OCT scans with a 30° field-of-view centered at the optic nerve head (ONH) as well as horizontal OCT scans were used for the analyses of structural changes. For single scans, 25 OCT scans were averaged.

In addition, a volume cube consisting of 49 single scans centered on the optic disc was recorded with a 30° field-of-view centered on the ONH. For each scan of the volume cube, nine OCT scans were averaged. This volume scan was used to calculate a retinal thickness map across the scanned retinal area. Thereby, the four circular inner subfields at 3-mm diameter around the central field surrounding the ONH were used, whereas the central (used for alignment of the ONH) and the outer (out of range due to the curvature of the small size of the eyes) subfields were excluded.

For the overview staining at the final time point, the eyes were dehydrated, embedded in paraffin, and 5-μm-thick transverse sections were cut and stained with hematoxylin and eosin (H&E; Sigma-Aldrich).

Functional measurement

Visual function was assessed using the OptoMotry system (CerebralMechanics, Lethbridge, AB, Canada) as described previously [22]. The optokinetic reflex (OKR) was thereby measured at baseline (BL), three days after $NaIO_3$ injection, and on 7, 14, 21, and 28 days PT. The system comprises a virtual 3-D cylinder on which vertical sine wave grating as visual stimuli was presented. Speed of rotation and geometry of the cylinder as well as spatial frequency of the stimuli were controlled by the OptoMotry© software. The direction of the grating rotation (clockwise vs. counter-clockwise) was randomly chosen by the software and allowed for separate measurement of the eyes. The test animal moving unrestrained on the centered platform tracked the grating with reflexive head movements. Two independent observers assessed via live video image the tracking movement. The spatial frequency of the grating was randomly increased (staircase procedure) during the session until the animal no longer responded. The highest spatial frequency that the mouse could track was identified as the threshold by the software.

Statistics

The data are presented as the mean ± SD, and were compared using SigmaPlot 12.0 (Systat Software, Erkrath, Germany) and the Kruskal–Wallis One Way ANOVA with post-hoc analysis by the Tukey test. For comparison of two groups, the Student's t test was applied. Differences were considered statistically significant at $P \leq 0.05$.

Results:

Differentiation of $CD45^-$ BMSCs in vitro

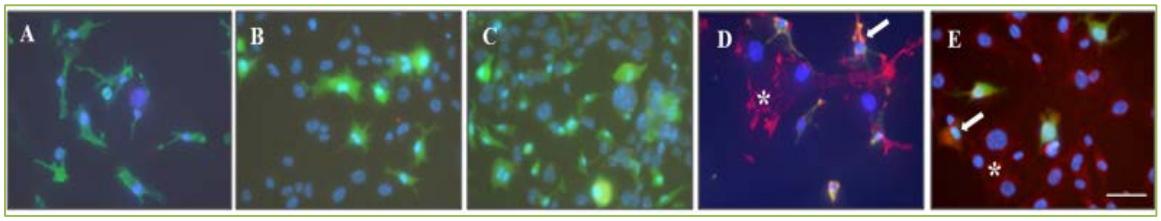

Figure 2. Predifferentiation of CD45$^-$ BMSC after coculture with mouse RPE. Staining of GFP$^+$ CD45$^-$ BMSCs on the RPE feeder layer for different lineage-specific markers on culture day 10. BMSCs were negative for the glia marker GFAP (Panel A) as well as the neuronal markers MAP-2 (Panel B) and βIII-tubulin (Panel C), but positive for the RPE markers RPE65 (Panel D) and bestrophin (Panel E). The markers are visualized in red, whereas GFP is seen in green. Examples of double-positive cells are marked with arrows, and positive RPE feeder cells are indicated by an asterisk. Bar represents 50 μm.

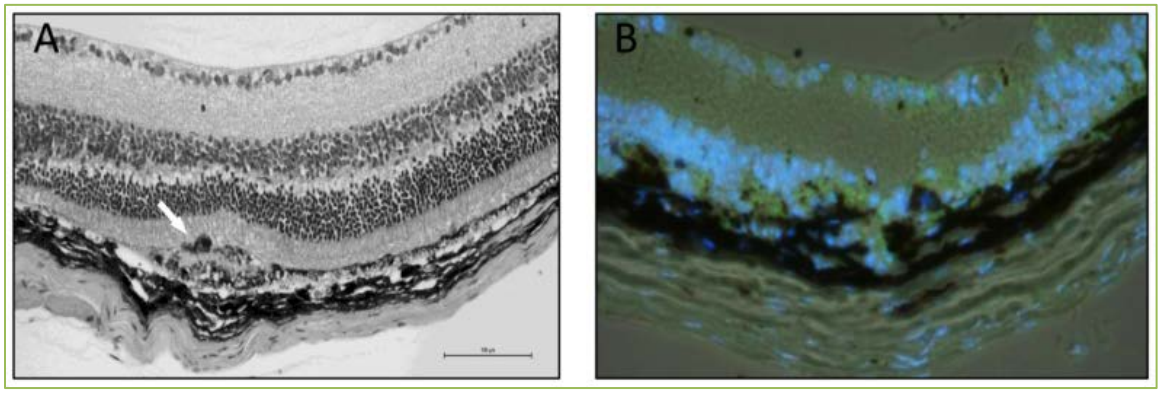

Figure 3. Visualization of subretinally transplanted BMSCs. Panel A shows a representative example of successful subretinal placement of BMSCs (arrow) via the scleral approach. The cells can be identified by their GFP labeling (green) as seen in panel B. The retinal structure was made visible by Nomarski optics. The bar represents 100 μm.

During coculture, the BMSCs changed their shape from a small, round appearance to a more elongated, epithelial-like morphology (Figure 1). Thereby, we observed a cell survival rate of 30–40%, and 70.8 ± 4.4% of the GFP-positive cells displayed morphological changes. The CD45$^-$ BMSCs showed no expression of the glia marker GFAP, the early neuronal marker βIII- tubulin or the late neuronal marker MAP-2 after coculture with RPE. However, the pre-differentiated BMSCs were positively stained for the RPE markers RPE65 and bestrophin (Figure 2).

Subretinal transplantation

BMSCs were harvested from the cocultures before transplantation and enriched by FACS using the FL1 fluorescence channel to separate GFP$^+$ cells. To avoid contamination by feeder cells that had taken up GFP, the sorting parameters were selected with appropriate controls (cultured feeder cells and GFP$^+$/GFP$^-$ bone marrow cells). The yield of sorted GFP$^+$ cells after coculture reached 44 ± 15% of the cell input. Approximately 60,000 pre-committed GFP$^+$ BMSCs were then transplanted into the subretinal space of mice with $NaIO_3$-induced retinal degeneration with a success rate of 79% (Figure 3A). The transplanted cells could be identified by their GFP expression (Figure 3B).

To monitor transplant location and retinal development, FAF and SD-OCT images were taken at different time points (Figure 4). At BL, before $NaIO_3$ treatment and subretinal transplantation, retina imaging showed a normal fundus in the IR image and a homogeneous FAF signal on the posterior pole of the eye. The SD-OCT images, which were simultaneously taken, also showed normal retinal layering at that time point (Figure 4A). After transplantation, GFP$^+$ BMSCs could be visualized using FAF and SD-OCT. The transplants appeared as an inhomogeneous, focal hyperfluorescent FAF signal, and the simultaneously taken SD-OCT images showed a corresponding subretinal deposit in the area of the hyperfluorescent FAF signal at day 28 PT (Figure 4B).

Visual function

Functional measurements using the OKR revealed a significant decrease in visual acuity after treatment with $NaIO_3$. Measurements after transplantation of pre-differentiated BMSCs did not show significant functional rescue over time (Table 2). However, 33% of the animals

Table 2. Visual acuity [c/°] after transplantation of pre-differentiated GFP$^+$ CD45$^-$ bone marrow-derived stem cells (BMSC) in the right eye (OD) of a mouse with $NaIO_3$-induced retinal degeneration (n = 15). The contralateral eye (OS) served as the internal control. The data are depicted as mean ± SD.

Time post transplantation	BMSC	
	OD	OS
Baseline	0.381 ± 0.003	0.380 ± 0.003
$NaIO_3$	0.291 ± 0.035 *	0.290 ± 0.037 *
Day 7	0.276 ± 0.053	0.288 ± 0.043
Day 14	0.278 ± 0.061	0.291 ± 0.058
Day 21	0.281 ± 0.060	0.301 ± 0.053
Day 28	0.281 ± 0.060	0.293 ± 0.060

* Significant at P ⩽ 0.05 vs. baseline.

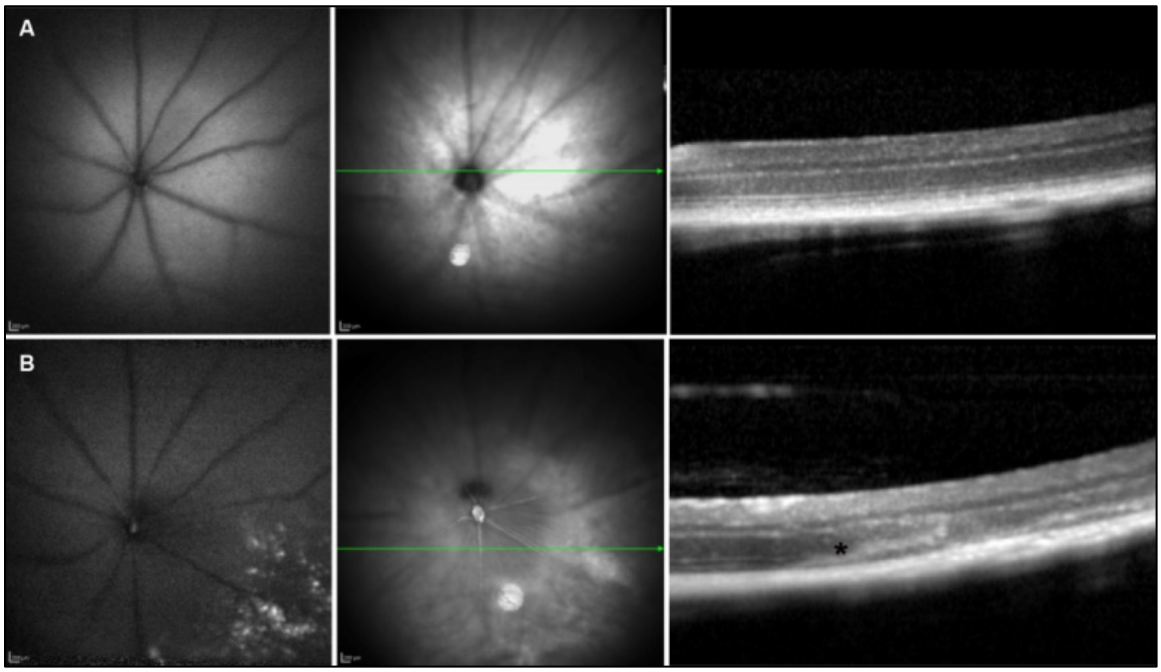

Figure 4. Images of the mouse retina at baseline before (A) and 28 days after (B) $NaIO_3$ treatment and transplantation. FAF mode (left) and IR SLO images (center) including the axis of the vertical OCT scan (right) are shown. The transplanted GFP$^+$ CD45$^-$ BMSCs are visible in the FAF modus (left). The corresponding OCT (center: IR SLO image) scan shows the transplant as a subretinal band-like deposit (right, asterisk).

showed improved visual acuity to a certain degree. The mean increase in visual acuity compared to the control eye was 24%.

Thickness measurements

To investigate possible rescue effects related to the subretinal BMSC transplantation, quantification of the retinal thickness using the OCT was conducted. The values were compared between sham-operated control (left eye - OS) and subretinal transplantation (right eye - OD) at different time points. The measured thickness after $NaIO_3$ showed significant thinning compared with the baseline in both groups. The retina of the transplanted eyes was further thinned compared with the control after 28 days. However, no statistically significant changes were found and the values after transplantation did not reach the values at baseline (Figure 5).

In vivo differentiation

IHC was performed to visualize *in vivo* differentiation of the transplanted BMSCs, and the transplants could be identified in the subretinal space by their GFP expression. The cells were found mainly in the outer retina but also in the ganglion cell layer, indicating migration through the sensory retina. Transplanted BMSCs were frequently positive for the RPE marker RPE65 (Figure 6). Thereby, the sensory retina above the differentiated BMSC appeared to be preserved (Figure 6A). Additionally, we found transplanted cells in proximity of remaining host RPE cells (Figure 6B). No positive staining for the glia marker GFAP or the neuronal lineage markers βIII- tubulin and MAP-2 were found in the transplanted BMSCs.

Discussion

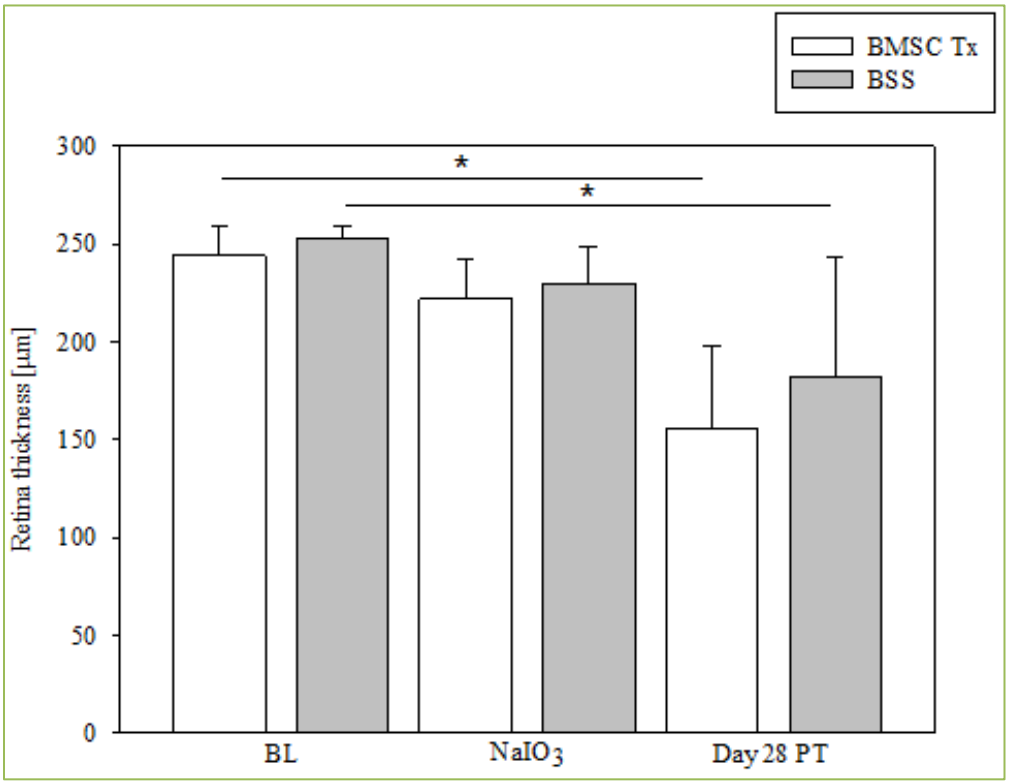

Figure 5. Measurement of ONL thickness by OCT. Volume scans were used to calculate a retinal thickness map across the scanned retinal area. Values of the four circular inner subfields at 3-mm diameter around the central field surrounding the ONH were averaged and compared to sham-operated control at different time points. Differences were considered significant at $P \leq 0.05$ (*, n = 7).

As damage to the RPE is a hallmark of AMD and one of the first pathophysiological events detectable replacement of the dysfunctional cells before irreversible atrophy of the foveal photoreceptors occurs was attempted [23, 24]. However, neither allogeneic nor autologous RPE transplantation has achieved morphological and/or functional rescue of the retina [3, 25]. One of the main hurdles for the successful clinical use of RPE transplantation is immune rejection despite the existence of ocular immune privilege [26]. Therefore, the use of BMSCs, which can be autologously harvested, has been pursued in recent years [27], and the focus is on the small population of tissue-specific stem cells shown by Kucia *et al*. (2004) [10]. The hypothesis is that enriching for BMSCs and their partial differentiation *in vitro* prior to transplantation may provide a viable, effective alternative for regeneration by SC. To this end, we were able to trigger early human BMSCs ($CD45^{-}CD38^{+}$) to morphologically and functionally progress along the RPE differentiation pathway *in vitro* [12]. Importantly, BMSCs can endogenously home to and incorporate into damaged RPE *in vivo* [13, 15]. These results point to the existence of SCs within the BM that are committed to the RPE lineage. There might be even an endogenous repair program to incorporate these cells into damaged RPE *in vivo*, which however cannot rescue the damaged structures efficiently.

In this study, we used BMSCs that were pre-differentiated *in vitro*. Thereby, differentiation of the SCs towards the RPE lineage, characterized by expression of RPE markers, has been achieved after coculture with RPE. Our results indicate that the RPE cells provide the specific cues for a directed stem cell differentiation towards the RPE lineage. Soluble factors secreted by the feeder cells and/or the direct cell-cell contact may be involved. For both hypotheses, examples can be found in the literature [13, 16]. Possible mechanisms underlying the plasticity of BMSCs have been summarized by Catacchio *et al*. (2013) [6]. Therefore, the need for a final clarification of the details, especially the characterization of modulating factors, is a tedious nevertheless necessary task beyond the scope of this study.

Because of the described direct coculture, the pre-differentiated BMSCs have to be separated and enriched before transplantation. The performed FACS for GFP-positive cells yielded a relatively low amount of transplantable cells. Furthermore, the procedure generates mechanical and environmental stress for the BMSCs, which could be one explanation for the rather limited effect of the subretinal cell transplantation on the visual acuity.

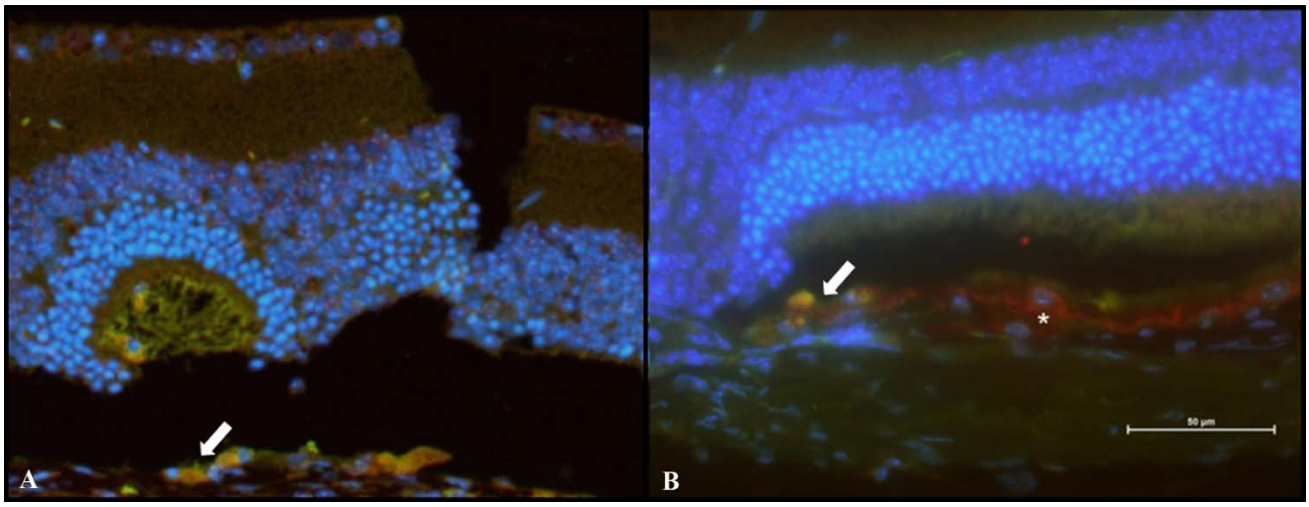

Figure 6. Staining for retinal markers in the mouse retina after $NaIO_3$ treatment and subretinal transplantation of BMSCs. The panels depict RPE65-positive BMSCs in the altered subretinal space of two different animals on post transplantation day 28. The white arrows mark double-positive cells in the transplantation area (green = GFP; red = RPE65), whereas the asterisk in panel B depicts remaining host RPE cells. The bar represents 50 μm.

Monitoring the fate of the transplants is pivotal for the follow-up of location, integration, and development of the donor cells, and can also be used to quantify the success of this regenerative approach. We were able to locate the GFP^+ BMSCs using OCT during all investigated time points up to day 28 PT. The cells appeared as inhomogeneous, focal hyperfluorescent signals in the FAF images and as subretinal deposits in the corresponding area in the simultaneously taken SD-OCT images. During the investigated time period, the quantity of fluorescent signals appeared to decrease, even if the distribution area of the transplants did not show significant changes. Moreover, non-fluorescent areas within the expanse of the transplant appeared at later time points. This could either be due to a decrease in the number of surviving cells or a decrease in the GFP intensity over time.

Functional visual recovery after cell transplantation is always the main goal of regenerative approaches in retinal degeneration. Our results showed improvements in the visual acuity in individual animals of both groups. A modest (1–4%) to relatively high (10–198%) increase in the visual acuity of the transplanted eye was measured, but it did not reach baseline values. However, this increase in visual acuity after BMSC transplantation might be due to secretion of neurostimulating factors. In this regard, pigment epithelium-derived factor (PEDF) appears to be a possible candidate as it displays neurotrophic properties [28]. Further studies would be needed to identify and characterize substances responsible for this effect. On the other hand, the majority of animals did not show an increase but rather a further decrease of their visual function. This might be due to the already initiated apoptosis in the photoreceptors that follows the initial damage of the RPE by $NaIO_3$ [29]. The impact of the subretinal surgery on the visual function should also be taken into account.

The BMSCs were found in the subretinal space where they constituted structures resembling a restricted monolayer or cell bolus. Some cells also migrated into the sensory retina and were found in the inner nuclear layer or even the ganglion layer. However, integration of the subretinal transplanted BMSCs in the retinal structure was rather limited. Mechanical destruction of the retinal structures during microsurgery and thereby activation of Müller cells might also have played a role in inducing gliosis and preventing better incorporation of the SCs [30].

Pre-committed BMSCs showed expression of the RPE marker RPE65 *in vitro* and then in the damaged subretinal space *in vivo.* None of the transplants showed positive staining for the neural markers. This indicates a RPE fate of the transplanted SCs indicating that specific cue can guide the differentiation path of a small population of BMSCs. However, too severe damage might prevent the stem cells from surviving in a deleterious environment and renders them unable to repair the damage.

Our data demonstrates that BMSCs were able to differentiate into RPE-like cells *in vitro* but did not repair the $NaIO_3$-induced retinal degeneration *in vivo*. This could be because of the pharmacological model of retinal degeneration ($NaIO_3$) that we used, the cell type (BMSC) that was introduced, or the route of delivery (subretinal transplantation). Even without complete rescue of retinal structure and function by the transplanted BMSCs, this concept shows viable results. In view of the advantages of

BMSCs, such as easy availability and the potential use of autologous cells in the human system, the approach should be investigated further. The experimental focus should be on better integration of the BMSCs, an increased number of pre-differentiated cells, and a more permissive microenvironment. Therefore, additional *in vitro* and *in vivo* experiments, including the utilization of human BMSCs, may bring more results regarding their potential use for retinal regeneration in degenerative diseases.

Acknowledgments

The authors thank Monika Kilchenmann, Sorin Ciocan, and Agathe Duda for their excellent technical assistance. This work was partly supported by grants from the Swiss National Science Foundation (310000-119894), the Velux Foundation, and the Berne University Research Foundation.

Conflict of interest

The authors declare that they have no conflicting interests.

References

1. Gouras P, Algvere PV. Retinal cell transplantation in the macula: new techniques. Vis Res 1996; 36:4121-4125.
2. Tezel TH, Del Priore LV, Kaplan HJ. Fate of human retinal pigment epithelium seeded onto layers of human Bruch's membrane. Invest Ophthalmol Vis Sci 1999; 40:467-476.
3. Del Priore LV, Geng L, Tezel TH, Kaplan HJ. Extracellular matrix ligands promote RPE attachment to inner Bruch's membrane. Cur Eye Res 2002; 25:79-89.
4. Phillips SJ, Sadda SR, Tso MO, Humayan MS, de Juan E, Jr., Binder S. Autologous transplantation of retinal pigment epithelium after mechanical debridement of Bruch's membrane. Curr Eye Res 2003; 26:81-88.
5. van Meurs JC, ter Averst E, Hofland L, van Hagen PM, Mooy CM, Baarsma GS, *et al*. Autologous peripheral retinal pigment epithelium translocation in patients with subfoveal neovascular membranes. Br J Ophthalmol 2004; 88:110-113.
6. Catacchio I, Berardi S, Reale A, De Luisi A, Racanelli V, Vacca A, *et al*. Evidence for bone marrow adult stem cell plasticity: properties, molecular mechanisms, negative aspects, and clinical applications of hematopoietic and mesenchymal stem cells transdifferentiation. Stem Cells Int 2013; 2013:589139.
7. Lin F, Cordes K, Li L, Hood L, Couser WG, Shankland SJ, *et al*. Hematopoietic stem cells contribute to the regeneration of renal tubules after renal ischemia-reperfusion injury in mice. J Am Soc Nephrol 2003; 14:1188-1199.
8. Harris JR, Brown GAJ, Jorgenson M, Kaushal S, Ellis EA, Grant MB, *et al*. Bone Marrow-Derived Cells Home to and Regenerate Retinal Pigment Epithelium after Injury. Invest Ophthalmol Vis Sci 2006; 47:2108-2113.
9. Orlic D, Kajstura J, Chimenti S, Jakoniuk I, Anderson SM, Li B, *et al*. Bone marrow cells regenerate infarcted myocardium. Nature 2001; 410:701-705.
10. Kucia M, Ratajczak J, Reca R, Janowska-Wieczorek A, Ratajczak MZ. Tissue-specific muscle, neural, and liver stem/progenitor cells reside in the bone marrow, respond to an SDF-1 gradient and are mobilized into peripheral blood during stress and tissue injury. Blood Cells Mol Dis 2004; 32:52-57.
11. Liu Y, Gao L, Zuba-Surma EK, Peng X, Kucia M, Ratajczak MZ, *et al*. Identification of small Sca-1(+), Lin(-), CD45(-) multipotential cells in the neonatal murine retina. Exp Hematol 2009; 37:1096-1107, 1107 e1091.
12. Mathivanan I, Trepp C, Brunold C, Baerlocher G, Enzmann V. Retinal differentiation of human bone marrow-derived stem cells by co-culture with retinal pigment epithelium in vitro. Exp Cell Res 2015; 333:11-20.
13. Li Y, Atmaca-Sonmez P, Schanie CL, Ildstad ST, Kaplan HJ, Enzmann V. Endogenous bone marrow derived cells express retinal pigment epithelium cell markers and migrate to focal areas of RPE damage. Invest Ophthalmol Vis Sci 2007; 48:4321-4327.
14. Atmaca-Sonmez P, Li Y, Yamauchi Y, Schanie CL, Ildstad ST, Kaplan HJ, *et al*. Systemically transferred hematopoietic stem cells home to the subretinal space and express RPE-65 in a mouse model of retinal pigment epithelium damage. Exp Eye Res 2006; 83:1295-1302.
15. Machalinska A, Klos P, Baumert B, Baskiewicz M, Kawa M, Rudnicki M, *et al*. Stem Cells are mobilized from the bone marrow into the peripheral circulation in response to retinal pigment epithelium damage--a pathophysiological attempt to induce endogenous regeneration. Cur Eye Res 2011; 36:663-672.
16. Duan P, Xu H, Zeng Y, Wang Y, Yin ZQ. Human Bone Marrow Stromal Cells can Differentiate to a Retinal Pigment Epithelial Phenotype when Co-Cultured with Pig Retinal Pigment Epithelium using a Transwell System. Cell Physiol Biochem 2013; 31:601-613.
17. Huang C, Zhang J, Ao M, Li Y, Zhang C, Xu Y, *et al*. Combination of Retinal Pigment Epithelium Cell-Conditioned Medium and Photoreceptor Outer Segments Stimulate Mesenchymal Stem Cell Differentiation Toward a Functional Retinal Pigment Epithelium Cell Phenotype. J Cell Biochem 2012; 113:590-598.
18. Machalinska A, Lubinski W, Klos P, Kawa M, Baumert B, Penkala K, *et al*. Sodium Iodate Selectively Injuries the Posterior Pole of the Retina in a Dose-Dependent Manner: Morphological and Electrophysiological Study. Neurochem Res 2010; 35:1819-1827.
19. Korte GE, Reppucci V, Henkind P. RPE destruction causes choriocapillary atrophy. Invest Ophthalmol Vis Sci 1984; 25:1135-1145.
20. Wang J, Iacovelli J, Spencer C, Saint-Geniez M. Direct effect of sodium iodate on neurosensory retina. Invest Ophthalmol Vis Sci 2014; 55:1941-1953.
21. Enzmann V, Row BW, Yamauchi Y, Kheirandish L, Gozal D, Kaplan HJ, *et al*. Behavioral and anatomical abnormalities in a sodium iodate-induced model of retinal pigment epithelium degeneration. Exp Eye Res 2006; 82:441-448.
22. Franco LM, Zulliger R, Wolf-Schnurrbusch UE, Katagiri Y, Kaplan HJ, Wolf S, *et al*. Decreased visual function after patchy loss of retinal pigment epithelium induced by low-dose sodium

iodate. Invest Ophthalmol Vis Sci 2009; 50:4004-4010.

23. Eldred GE. Lipofuscin fluorophore inhibits lysosomal protein degradation and may cause early stages of macular degeneration. Gerontology 1995; 41:15-28.
24. Kunze C, Elsner AE, Beausencourt E, Moraes L, Hartnett ME, Trempe CL. Spatial extent of pigment epithelial detachments in age-related macular degeneration. Ophthalmology 1999; 106:1830-1840.
25. Phillips SJ, Sadda SR, Tso MOM, Humayun MS, de Juan E, Jr., Binder S. Autologous transplantation of RPE after mechanical debridement of Bruch's membrane. Cur Eye Res 2003; 26:81-88.
26. Enzmann V, Faude F, Wiedemann P, Kohen L. Immunological problems of transplantation into the subretinal space. Acta Anat 1998; 162:178-183.
27. Enzmann V, Yolcu E, Kaplan HJ, Ildstad ST. Stem cells as tools in regenerative therapy for retinal degeneration. Arch Ophthalmol 2009; 127:563-571.
28. Malchiodi-Albedi F, Feher J, Caiazza S, Formisano G, Perelli R, Falchi M, *et al*. PEDF (pigment epithelium-derived factor) promotes increase and maturation of pigment granules in pigment epithelial cells in neonatal albino rat retinal cultures. Int J Dev Neurosci 1998; 16:423-432.
29. Kiuchi K, Yoshizawa K, Shikata N, Moriguchi K, Tsubura A. Morphological characteristics of retinal degeneration induced by sodium iodate in mice. Cur Eye Res 2002; 25:373-379.
30. Bringmann A, Iandiev I, Pannicke T, Wurm A, Hollborn M, Wiedemann P, *et al*. Cellular signaling and factors involved in Muller cell gliosis: Neuroprotective and detrimental effects. Prog Retin Eye Res 2009; 28:423-451.

Supplemental figure S1

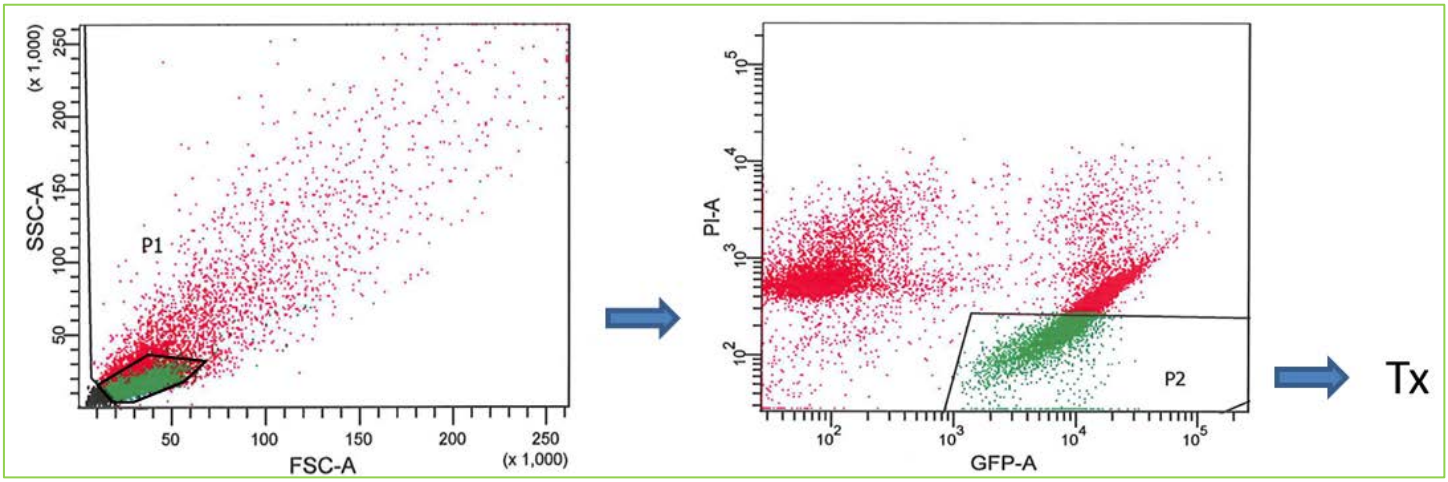

Supplemental figure 1. Sorting strategy for the separation of BMSCs from the RPE feeder cells by FACS after co-culture. Murine BMSCs were identified with FSC vs. SSC signals according to their size within the lymphoid gate (P1). Further sorting was performed by excluding dead cells [Propidium iodide (PI) positive cells] and selecting GFP-positive cells (P2). The selected cells were then subretinally transplanted (Tx).